

Article

Improving Mechanical Oscillator Cooling in a Double-Coupled Cavity Optomechanical System with an Optical Parametric Amplifier

Peipei Pan, Aixi Chen  and Li Deng *

School of Science, Zhejiang Sci-Tech University, Hangzhou 310018, China; 202020103089@mails.zstu.edu.cn (P.P.); aixichen@zstu.edu.cn (A.C.)

* Correspondence: lideng75@zstu.edu.cn

Abstract: We investigate the cooling phenomenon of a mechanical oscillator in a double-coupled cavity optomechanical system. Our model includes two single-mode optical cavities. The left cavity is an optomechanical system with an optical parametric amplifier, and the right cavity is a standard optical cavity. The two optical cavities couple with each other by exchanging photons. The optomechanical system is effectively driven by an input laser field. By solving the linear quantum Langevin equation of the system under a steady-state condition, we can obtain the position fluctuation spectrum and momentum fluctuation spectrum of the mechanical oscillator, and then, the expression of its effective temperature is obtained. Through numerical analysis, we find the change in the effective temperature of the mechanical oscillator under different physical parameters. The results show that the cooling of the mechanical oscillator can be significantly improved in the presence of optical parameter amplification and adjustment of optical cavity parameters. Our cooling solutions have potential applications for the preparation of nonclassical states of mechanical oscillators, high-precision measurements, and quantum information processing.

Keywords: cooling of the mechanical oscillator; optomechanical system; optical parametric amplifier

MSC: 81V80



Citation: Pan, P.; Chen, A.; Deng, L. Improving Mechanical Oscillator Cooling in a Double-Coupled Cavity Optomechanical System with an Optical Parametric Amplifier.

Mathematics **2023**, *11*, 2218. <https://doi.org/10.3390/math11092218>

Academic Editor: Dmitry Makarov

Received: 16 April 2023

Revised: 3 May 2023

Accepted: 5 May 2023

Published: 8 May 2023



Copyright: © 2023 by the authors. Licensee MDPI, Basel, Switzerland. This article is an open access article distributed under the terms and conditions of the Creative Commons Attribution (CC BY) license (<https://creativecommons.org/licenses/by/4.0/>).

1. Introduction

In theoretical and experimental fields, the cavity optomechanical system [1,2] has attracted extensive attention for its wide applications, such as the high-precision detection of gravitational waves and mass [3,4], mechanical entanglement [5], biological sensing [6], mechanical squeezing [7,8], mechanical displacement [9], quantum information processing [10], and superpositions of macroscopic quantum states [11]. The research on optomechanical systems shows that people can use photons, nonclassical states, and mechanical motion to manipulate and measure quantum effects in quantum regions. The optomechanical system can constitute a hybrid quantum system [12,13] with other different physical systems, providing a new approach for us to explore the quantum world. A specific optomechanical system is mainly composed of a mechanical oscillator and cavity. In order to observe and measure the quantum effect of macroscopic mechanical systems experimentally, it is necessary to overcome the thermal noise of the mechanical oscillator and prepare it in the quantum ground state [14]. Therefore, exploring mechanical oscillator cooling becomes a crucial adjective, which could be achieved in the optomechanical system, enhancing the interaction between the optical field and the mechanical motion to reduce the thermal noise [15].

Currently, considerable progress has been made in the cooling of mechanical oscillators. Generally, the most frequently used methods are self-cooling [16–22] and active feedback cooling [23–27]. In the active feedback cooling schemes, a viscous force is applied to a

mechanical oscillator by measuring its position without generating thermal noise. However, the measurement accuracy of this method is affected by noise in the feedback loop. The self-cooling scheme is to achieve cooling by interacting with the mechanical oscillator and auxiliary system and absorbing energy from the mechanical oscillator. Resolved sideband cooling [28–30] is a universal study in self-cooling scheme. However, the precondition of this scheme is that the dissipation coefficient of the optical cavity is much smaller than the frequency of the mechanical oscillator, which has high requirements for the quality factor of the optical cavity. Later, people began to explore mechanical oscillator cooling under unresolved sideband conditions. For example, Guo et al. used electromagnetically induced transparency to break through the limitation of the unresolved conditions of the sideband on the fluctuation spectrum of light pressure [31]. Furthermore, Liu et al. demonstrated that the motional ground state can be achieved in the highly unresolved sideband regime through coherent auxiliary cavity interferences [32].

Cooling mechanical oscillators to lower temperatures has become a greater focus. A degenerate optical parametric amplifier [33] has been shown to improve the cooling of mechanical oscillators. For instance, Huang et al. used parametric to enhance the cavity cooling of a micromechanical mirror in the dispersive coupling [34]. Further, they investigated the cooling of the mechanical membrane in a dissipative optomechanical system with a degenerate optical parametric amplifier [35]. Researchers have demonstrated that coupling a degenerate optical parametric with a Fabry–Perot optical cavity can tremendously improve the cooling of the mechanical oscillator [22,34,36].

This paper analyzes the scheme for improving mechanical oscillator cooling in double-coupled cavity optomechanical systems with an optical parametric amplifier. The paper is organized as follows: Section 2 introduces the model of the system and provides the quantum Langevin equations. In Section 3, we calculate the position fluctuation spectrum and momentum fluctuation spectrum of the mechanical oscillator and derive the effective temperature of the mechanical oscillator. In Section 4, we show the effective resonance frequency and effective damping rate of the mechanical oscillator, and we also represent how the cooling of the mechanical oscillator can be effectively improved by using an optical parametric amplifier inside the cavity alongside adjusting the optical cavity parameters. Some conclusions are presented in Section 5.

2. Model

The model that we consider is a coupled single-mode double-cavity, as shown in Figure 1. The left and right optical cavities are cavity a_1 and cavity a_2 , respectively. The left cavity is an optomechanical system and the right cavity is a standard optical cavity. The two cavities are coupled to each other through photon exchange coupling with the coupling coefficient J . A degenerate optical parametric amplifier is placed in the left cavity. The resonance frequency and decay rate of the left cavity are ω_1 and κ_1 , respectively, and the resonance frequency and decay rate of the right cavity are ω_2 and κ_2 , respectively. The movable cavity mirror in the left cavity can be regarded as a mechanical oscillator with a natural frequency of ω_m , effective mass m , and damping rate γ_m . The system is in a state of thermal equilibrium at temperature T . In addition, the left cavity is driven with an input laser field with frequency ω_L , power P and amplitude ε , which does not interact directly with the right cavity.

Therefore, the Hamiltonian of the system under the rotational frame of the input laser frequency ω_L can be expressed as:

$$\begin{aligned}
 H = & \hbar\Delta_1 a_1^\dagger a_1 + \hbar\Delta_2 a_2^\dagger a_2 + \frac{1}{2} \left(\frac{p^2}{m} + m\omega_m^2 q^2 \right) - \hbar g a_1^\dagger a_1 q + \hbar J (a_1^\dagger a_2 + a_1 a_2^\dagger) \\
 & + i\hbar\varepsilon (a_1^\dagger - a_1) + i\hbar G (e^{i\theta} a_1^{\dagger 2} - e^{-i\theta} a_1^2).
 \end{aligned}
 \tag{1}$$

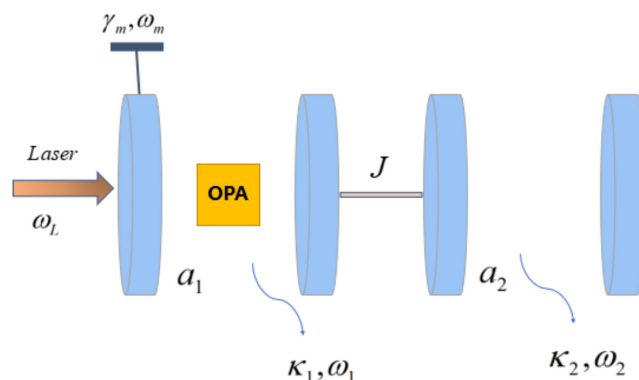


Figure 1. Model diagram of a dual-cavity optomechanical coupling system. The two optical cavities interact through the coupling coefficient J . A degenerate optical parametric amplifier is placed in the left cavity. The leftmost movable cavity mirror can be regarded as a mechanical oscillator with a resonance frequency of ω_m . The left cavity is driven by a laser field.

Here a_1 and a_1^\dagger are the annihilation and creation operators for the field inside the left cavity, respectively, and a_2 and a_2^\dagger are the annihilation and creation operators for the field inside the right cavity, respectively, which satisfy the commutative relationship $[a_j, a_j^\dagger] = 1 (j = 1, 2)$. $\Delta_1 = \omega_1 - \omega_L$, where $\Delta_2 = \omega_2 - \omega_L$ are the detuning of the left cavity and the right cavity to the input laser, respectively. Further, p and q are the momentum and position operators of the movable cavity mirror, respectively, satisfying $[q, p] = i\hbar$. While $g = \omega_1/L$ is the single-photon optomechanical coupling coefficient, and L is the length of the two cavities. Then, $\mathcal{E} = (2\kappa_1 P/\hbar\omega_L)^{1/2}$ is the amplitude of the input laser, G is the nonlinear gain of the OPA, and θ is the drive field phase of the OPA. In Equation (1), the first two terms represent the energy of the left cavity and the right cavity, respectively, the third term represents the energy of the mechanical oscillator, the fourth term represents the interaction between the mechanical oscillator and the left cavity, the fifth term represents the interaction between the left cavity and the right cavity, the sixth term represents the interaction between the left cavity and the input driving light, and the last term represents the interaction between the left cavity and OPA. The quantum Langevin equation of the system can be provided by the Heisenberg equation:

$$\begin{aligned}
 \dot{q} &= \frac{p}{m}, \\
 \dot{p} &= -m\omega_m^2 q + \hbar g a_1^\dagger a_1 - \gamma_m p + \xi, \\
 \dot{a}_1 &= -(i\Delta_1 + \kappa_1)a_1 + i g a_1 q - i J a_2 + 2G e^{i\theta} a_1^\dagger + \varepsilon + \sqrt{2\kappa_1} a_{1,in}, \\
 \dot{a}_2 &= -(i\Delta_2 + \kappa_2)a_2 - i J a_1 + \sqrt{2\kappa_2} a_{2,in}.
 \end{aligned}
 \tag{2}$$

Here, we introduce the input vacuum noise operators $a_{1,in}$ and $a_{2,in}$ with zero mean values, and the relevant equations in the time domain are [37]:

$$\begin{aligned}
 \langle \delta a_{1,in}(t) \delta a_{1,in}^\dagger(t') \rangle &= \delta(t - t'), \\
 \langle \delta a_{1,in}(t) \delta a_{1,in}(t') \rangle &= \langle \delta a_{1,in}^\dagger(t) \delta a_{1,in}^\dagger(t') \rangle = 0, \\
 \langle \delta a_{2,in}(t) \delta a_{2,in}^\dagger(t') \rangle &= \delta(t - t'), \\
 \langle \delta a_{2,in}(t) \delta a_{2,in}(t') \rangle &= \langle \delta a_{2,in}^\dagger(t) \delta a_{2,in}^\dagger(t') \rangle = 0.
 \end{aligned}
 \tag{3}$$

Due to the interaction between the mechanical oscillator and the thermal bath, a force ζ will be generated, which is a Brownian noise operator, and its mean value is also zero, and the relevant equation satisfied is [38]:

$$\langle \zeta(t)\zeta(t') \rangle = \frac{\hbar\gamma_m m}{2\pi} \int \omega e^{-i\omega(t-t')} \left[\coth\left(\frac{\hbar\omega}{2k_B T}\right) + 1 \right] d\omega, \tag{4}$$

where k_B is the Boltzmann constant and T is the bath temperature. By setting all-time derivatives of the quantum Langevin equation to zero, we can obtain the steady state average of the system:

$$\begin{aligned} p_s &= 0, \\ q_s &= \frac{\hbar g |a_{1s}|^2}{m\omega_m^2}, \\ a_{2s} &= \frac{-iJ a_{1s}}{i\Delta_2 + \kappa_2}, \\ a_{1s} &= \frac{2Ge^{i\theta} \varepsilon (\Delta_2^2 + \kappa_2^2) + \varepsilon (i\Delta_2 + \kappa_2) [(\kappa_1 - i\Delta)(\kappa_2 - i\Delta_2)]}{(\kappa_1^2 + \Delta^2)(\kappa_2^2 + \Delta_2^2) + 2J^2(\kappa_1\kappa_2 - \Delta\Delta_2) + J^4 - 4G^2(\kappa_2^2 + \Delta_2^2)}. \end{aligned} \tag{5}$$

Here a_{1s} and a_{2s} represent the steady-state amplitude of the two cavity fields, respectively. Moreover, $\Delta = \Delta_1 - gq_s$ is the detuning of the effective cavity, which is generated under the influence of the radiation pressure and is related to the average displacement of the mechanical oscillator. We can see that $q_s \neq 0$, indicating that after adding a series of coupled systems, the mechanical oscillator is moved around the new equilibrium position.

3. Radiation Pressure and Quantum Fluctuations

Since the fluctuation $\delta q = q - q_s$ is the real operator of the mechanical oscillator, and it is also the object that is processed by cooling the mechanical oscillator, we first define all the fluctuation operators of the system:

$$\delta q = q - q_s, \delta p = p - p_s, \delta a_1 = a_1 - a_{1s}, \delta a_2 = a_2 - a_{2s}. \tag{6}$$

Substituting the fluctuation operator into the equation, we can get the linear quantum Langevin equation:

$$\begin{aligned} \delta \dot{q} &= \frac{\delta p}{m}, \\ \delta \dot{p} &= -m\omega_m^2 \delta q + \hbar g (a_{1s} \delta a_1^\dagger + a_{1s}^* \delta a_1) - \gamma_m \delta p + \zeta, \\ \delta \dot{a}_1 &= -(i\Delta + \kappa_1) \delta a_1 + i g a_{1s} \delta q - i J \delta a_2 + 2G e^{i\theta} \delta a_1^\dagger + \sqrt{2\kappa_1} a_{1,in}, \\ \delta \dot{a}_2 &= -(i\Delta_2 + \kappa_2) \delta a_2 - i J \delta a_1 + \sqrt{2\kappa_2} a_{2,in}. \end{aligned} \tag{7}$$

Here we introduce the quadrature for the two cavity fields $\delta x_1 = \delta a_1 + \delta a_1^\dagger$, $\delta y_1 = i(\delta a_1^\dagger - \delta a_1)$ and $\delta x_2 = \delta a_2 + \delta a_2^\dagger$, $\delta y_2 = i(\delta a_2^\dagger - \delta a_2)$, alongside the input noise quadrature operator: $x_{1,in} = a_{1,in} + a_{1,in}^\dagger$, $y_{1,in} = i(a_{1,in}^\dagger - a_{1,in})$ and $x_{2,in} = a_{2,in} + a_{2,in}^\dagger$, $y_{2,in} = i(a_{2,in}^\dagger - a_{2,in})$. Equation (7) can be expressed in matrix form:

$$\dot{A}(t) = MA(t) + \eta(t), \tag{8}$$

here $A(t)$ is a column vector of fluctuations, $\eta(t)$ is a column vector of noise terms, and their transpose can be written as:

$$\begin{aligned} A(t)^T &= (\delta q, \delta p, \delta x_1, \delta y_1, \delta x_2, \delta y_2), \\ \eta(t)^T &= (0, \zeta, \sqrt{2\kappa_1} x_{1,in}, \sqrt{2\kappa_1} y_{1,in}, \sqrt{2\kappa_2} x_{2,in}, \sqrt{2\kappa_2} y_{2,in}). \end{aligned} \tag{9}$$

The matrix M is represented as:

$$\begin{pmatrix} 0 & \frac{1}{m} & 0 & 0 & 0 & 0 \\ -m\omega_m^2 & -\gamma_m & \hbar\phi & \hbar\psi & 0 & 0 \\ -2\psi & 0 & -(\kappa_1 - 2G \cos \theta) & \Delta + 2G \sin \theta & 0 & J \\ 2\phi & 0 & -\Delta + 2G \sin \theta & -(\kappa_1 + 2G \cos \theta) & -J & 0 \\ 0 & 0 & 0 & J & -\kappa_2 & \Delta_2 \\ 0 & 0 & -J & 0 & -\Delta_2 & -\kappa_2 \end{pmatrix}, \tag{10}$$

here $\phi = g(a_{1s} + a_{1s}^*)/2$ and $\psi = g(a_{1s} - a_{1s}^*)/2i$. The solution of Equation (7) is stable when all the eigenvalues of the matrix have negative real parts. According to the Rouse-Hurwitz stability criterion [39], we can obtain the stability condition. Since it is too complicated, it will not be shown here, and we will perform numerical simulations on the parameters we selected in order to satisfy the stability conditions. By performing the Fourier transform on the formula, we obtain the position fluctuation of the mechanical oscillator in the frequency domain:

$$\delta q(\omega) = \chi(\omega)[A_1(\omega)a_{1,in}(\omega) + A_2(\omega)a_{1,in}^+(\omega) + A_3(\omega)a_{2,in}(\omega) + A_4(\omega)a_{2,in}^+(\omega) + Z(\omega)\zeta(\omega)], \tag{11}$$

where

$$\begin{aligned} \chi^{-1}(\omega) &= m(\omega_m^2 - i\omega\gamma_m - \omega^2)Z(\omega) - i\hbar|g_0|^2[v_+(u_-v_- + J^2) - v_-(u_+v_+ + J^2)] \\ &\quad - 2i\hbar Gv_+v_-(g_0^2e^{-i\theta} - g_0^{*2}e^{i\theta}), \\ Z(\omega) &= (u_+v_+ + J^2)(u_-v_- + J^2) - 4G^2v_+v_-, \quad g_0 = ga_{1s}, \quad g_0^* = ga_{1s}^*, \\ u_+ &= \kappa_1 - i\omega + i\Delta, \quad u_- = \kappa_1 - i\omega - i\Delta, \quad v_+ = \kappa_2 - i\omega + i\Delta_2, \quad v_- = \kappa_2 - i\omega - i\Delta_2, \\ A_1(\omega) &= 2\hbar g_0 G e^{-i\theta} v_+ v_- \sqrt{2\kappa_1} + \hbar g_0^* v_+ \sqrt{2\kappa_1} (u_- v_- + J^2), \\ A_2(\omega) &= 2\hbar g_0^* G e^{i\theta} v_+ v_- \sqrt{2\kappa_1} + \hbar g_0 v_- \sqrt{2\kappa_1} (u_+ v_+ + J^2), \\ A_3(\omega) &= -2i\hbar g_0 J G e^{-i\theta} v_- \sqrt{2\kappa_2} - iJ\hbar g_0^* (u_- v_- + J^2) \sqrt{2\kappa_2}, \\ A_4(\omega) &= 2i\hbar g_0^* J G e^{i\theta} v_+ \sqrt{2\kappa_2} + iJ\hbar g_0 (u_+ v_+ + J^2) \sqrt{2\kappa_2}. \end{aligned} \tag{12}$$

In Equation (11), the first four terms are caused by the input vacuum noise caused by mutual coupling in the system, and the last term is derived from the thermal noise in the environment. Here $\chi(\omega)$ is the susceptibility of the mechanical oscillator in the presence of the coupled system, which can be written as:

$$\chi(\omega) = \frac{1}{m[\omega_{eff}(\omega)^2 - i\omega\gamma_{eff}(\omega) - \omega^2]}, \tag{13}$$

where $\omega_{eff}(\omega)$ and $\gamma_{eff}(\omega)$ are the effective resonance frequency and effective damping rate of the mechanical oscillator, respectively, and they can be expressed as:

$$\begin{aligned} \omega_{eff}(\omega) &= \left\{ \omega_m^2 - \text{Re} \left[\frac{B_1(\omega) + B_2(\omega)}{mZ(\omega)} \right] \right\}^{\frac{1}{2}}, \\ \gamma_{eff}(\omega) &= \gamma_m + \text{Im} \left[\frac{B_1(\omega) + B_2(\omega)}{m\omega Z(\omega)} \right], \end{aligned} \tag{14}$$

here,

$$\begin{aligned} B_1(\omega) &= i\hbar|g_0|^2v_+(u_-v_- + J^2) - i\hbar|g_0|^2v_-(u_+v_+ + J^2), \\ B_2(\omega) &= 2i\hbar Gv_+v_-(g_0^2e^{-i\theta} - g_0^{*2}e^{i\theta}). \end{aligned} \tag{15}$$

We note that the effective resonance frequency $\omega_{eff}(\omega)$ and the effective damping rate $\gamma_{eff}(\omega)$ of the mechanical oscillator are related to the enhanced optomechanical coupling

coefficient, the parametric gain coefficient G of the OPA, and the phase θ . In the case of an uncoupled system ($g = 0$), the mechanical oscillator performs Brownian motion, and its effective susceptibility $\chi(\omega) = m^{-1}(\omega_m^2 - i\omega\gamma_m - \omega^2)^{-1}$ is a standard Lorentzian function [40]. The position fluctuation spectrum of the mechanical oscillator is defined as:

$$2\pi S_q(\omega)\delta(\omega + \Omega) = \frac{1}{2}[\langle \delta q(\omega)\delta q(\Omega) \rangle + \langle \delta q(\Omega)\delta q(\omega) \rangle], \tag{16}$$

whereby we introduce the non-zero correlation of the noise term in the frequency domain:

$$\begin{aligned} \langle a_{1,in}(\omega)a_{1,in}^\dagger(-\Omega) \rangle &= 2\pi\delta(\omega + \Omega), \\ \langle a_{2,in}(\omega)a_{2,in}^\dagger(-\Omega) \rangle &= 2\pi\delta(\omega + \Omega), \\ \langle \zeta(\omega)\zeta(\Omega) \rangle &= 2\pi\hbar\gamma_m m\omega \left[1 + \coth\left(\frac{\hbar\omega}{2k_B T}\right) \right] \delta(\omega + \Omega), \end{aligned} \tag{17}$$

then, we obtain the position fluctuation spectrum of the mechanical oscillator:

$$S_q(\omega) = \chi(\omega)\chi(-\omega) \left[A_{12}(\omega) + A_{34}(\omega) + \hbar m\omega\gamma_m Z(\omega)Z(-\omega)\coth\left(\frac{\hbar\omega}{2k_B T}\right) \right], \tag{18}$$

where

$$\begin{aligned} A_{12}(\omega) &= \frac{A_1(\omega)A_2(-\omega) + A_1(-\omega)A_2(\omega)}{2}, \\ A_{34}(\omega) &= \frac{A_3(\omega)A_4(-\omega) + A_3(-\omega)A_4(\omega)}{2}. \end{aligned} \tag{19}$$

In Equation (18), the first two terms are the contribution of the input vacuum noise, and the last term is the contribution of the thermal noise. When we take the Fourier transform of $\delta q = \delta p/m$ in Equation (7), we can get $S_p(\omega) = m^2\omega^2 S_q(\omega)$, which makes the momentum fluctuation spectrum of the mechanical oscillator $S_p(\omega) = m^2\omega^2 S_q(\omega)$. For a system in thermal equilibrium, we can use the energy equipartition theorem to define the effective temperature $k_B T_{eff} = m\omega_m^2 \langle q^2 \rangle / 2 + \langle p^2 \rangle / 2m$, which is determined by the total energy of the mechanical oscillator. Note, we are dealing with a drive system here, and $m\omega_m^2 \langle q^2 \rangle / 2 \neq \langle p^2 \rangle / 2m$ [34], where $\langle q^2 \rangle = \frac{1}{2\pi} \int_{-\infty}^{\infty} S_q(\omega) d\omega$, $\langle p^2 \rangle = \frac{1}{2\pi} \int_{-\infty}^{\infty} S_p(\omega) d\omega$. Through analysis, we find that the cooling of the mechanical oscillator is related to the decay rate, detuning, coupling coefficient, and OPA gain coefficient of the two cavities.

4. Results and Discussions

4.1. Effective Resonance Frequency and Effective Damping Rate of Mechanical Oscillator

Firstly, we show the effect of coupled dual cavity and OPA on the effective resonance frequency and effective damping rate of the mechanical oscillator. In the numerical calculations we have chosen some similar parameters that have been used in past experiments: $m = 145 \text{ ng}$, $L = 25 \text{ mm}$, $\omega_m / (2\pi) = 215 \text{ kHz}$, $P = 0.2 \text{ Mw}$, $\lambda_L = 2\pi c / \omega_L = 1064 \text{ nm}$, and mechanical quality factor $Q = \omega_m / \gamma_m = 8000$. We take the same value for the decay rate of the two cavities $\kappa_1 = \kappa_2 = \omega_m$; therefore, our system is in an unresolved sideband condition. We plotted the normalized effective resonance frequency $\omega_{eff}(\omega) / \omega_m$ and normalized effective damping rate $\gamma_{eff}(\omega) / \gamma_m$ of the mechanical oscillator versus the normalized frequency ω / ω_m for different coupling coefficients J and parametric gain G . We take the cavity detuning of the two cavities as $\Delta = 1.2\omega_m$, $\Delta_2 = 2\omega_m$, and the parametric phase $\theta = 0$.

In Figure 2, we fixed $J = 1.5\kappa_1$ and plotted the curves of the normalized effective resonance frequency $\omega_{eff}(\omega) / \omega_m$, which normalized the effective damping rate $\gamma_{eff}(\omega) / \gamma_m$ versus the normalized effective resonance frequency $\omega_{eff}(0) / \omega_m$, when $G = 0$ (red solid line), $G = 0.15\kappa_1$ (green solid line), and $G = 0.19\kappa_1$ (black solid line), respectively. According to Figure 2a,b, it can be seen that both the normalized effective resonance frequency and the normalized effective damping rate are symmetrically distributed within the se-

lected interval as the normalized effective frequency changes, and are symmetric about the longitudinal axis. When $G = 0$, there is no optical parametric amplifier placed in the left cavity. In Figure 2a, while ω is from $-7\omega_m$ to $-5\omega_m$ and from $5\omega_m$ to $7\omega_m$, the normalized effective resonance frequency of the mechanical oscillator remained basically unchanged. Then, as the value of ω increases in the left half-axis and decreases in the right half-axis, the normalized effective resonance frequency will suddenly decrease. When $\omega = 0$, the normalized effective resonance frequency has a minimum value. When an optical parametric amplifier is placed in the left cavity, the image of the normalized effective resonance frequency still shows a symmetrical distribution. However, the difference between this situation and the absence of an optical parametric amplifier in the cavity is that when the normalized effective resonance frequency reaches a subpeak, it rapidly decreases and reaches a minimum value. It is worth noting that when $G = 0.19\kappa_1$, its normalized effective resonance frequency is lower than the value when $G = 0.15\kappa_1$. In Figure 2b, when $G = 0$, the normalized effective damping rate of the mechanical oscillator shows three peaks in the selected region, with two subpeaks appearing at approximately $\omega = -3\omega_m$ and $\omega = 3\omega_m$, with the maximum value appearing at $\omega = 0$. However, the difference between the maximum and sub-maximum values is not significant, and as it extends along the left and right half axes, the value of the normalized effective damping rate gradually approaches zero. After adding OPA, the overall trend of the normalized effective damping rate is similar to without OPA, yet the difference is that the peak value of the normalized effective damping rate suddenly increases several times. Moreover, the peak value at $G = 0.19\kappa_1$ is greater than at $G = 0.15\kappa_1$, and it is found that this pattern corresponds to the normalized effective resonance frequency. That is, at $\omega = 0$, the larger the normalized effective frequency $\omega_{eff}(0)/\omega_m$ of the mechanical oscillator, the smaller its normalized effective damping rate $\gamma_{eff}(0)/\gamma_m$. Figure 2 also shows that with the increase of parameter gain G , the normalized effective resonance frequency $\omega_{eff}(0)/\omega_m$ decreases, while the normalized effective damping rate increases $\gamma_{eff}(0)/\gamma_m$. However, it is worth noting that a larger value of G is not necessarily better, which indicates that adding OPA to the dual cavity can effectively assist in the cooling of the mechanical oscillator. Similarly, we also selected $J = 1.25\kappa_1$, $\Delta = 0.9\omega_m$, and $\Delta_2 = 2\omega_m$, as well as the parameter phase $\theta = 0$, to observe the changes in the normalized effective resonance frequency and normalized effective damping rate of the mechanical oscillator by increasing the parameter gain G . As shown in Figure 3, it can be observed that the change in curves presented in Figure 3 is similar to Figure 2. In addition, the influence of the values on the normalized effective resonance frequency and normalized effective damping rate is also discussed. It is found that when $\theta = 2k\pi (k \in N)$, the normalized effective resonance frequency achieves the minimum value, while the normalized effective damping rate reaches the maximum value. Therefore, in the following discussion, we take $\theta = 0$ for simplicity.

4.2. Cooling the Mechanical Oscillator

We assumed that the initial environment temperature is $T = 300K$, which means that the thermal phonon number of the mechanical oscillator is $n_m^{th} = 2.90743 \times 10^7$, where $n_m^{th} = 1 / \{\exp[\hbar\omega_m / (k_B T)] - 1\}$. We plotted the relationship between the effective temperature of the mechanical oscillator and the normalized detuning Δ/ω_m of the left cavity. We fixed $J = 1.5\kappa_1$ and plotted the curves when $G = 0$, $G = 0.15\kappa_1$, and $G = 0.19\kappa_1$, respectively, as shown in Figure 4.

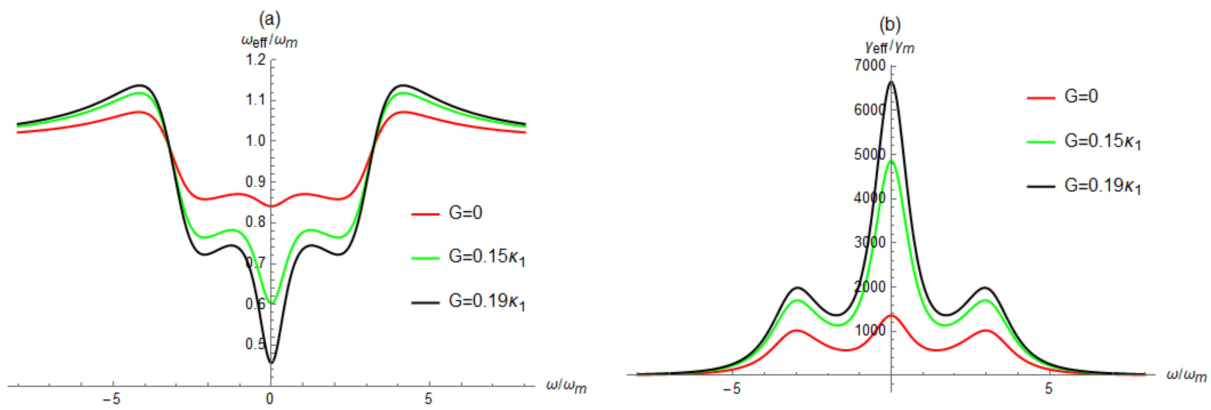


Figure 2. (a) The normalized effective resonance frequency $\omega_{eff}(\omega)/\omega_m$ of the mechanical oscillator as a function of the normalized frequency ω/ω_m for different parametric gains G ; (b) The normalized effective damping rate $\gamma_{eff}(\omega)/\gamma_m$ of the mechanical oscillator as a function of the normalized frequency ω/ω_m . The red curve, green curve, and black curve correspond to $G = 0$, $G = 0.15\kappa_1$, and $G = 0.19\kappa_1$, respectively. Where $\Delta = 1.2\omega_m$, $\Delta_2 = 2\omega_m$, $J = 1.5\kappa_1$, and $\theta = 0$.

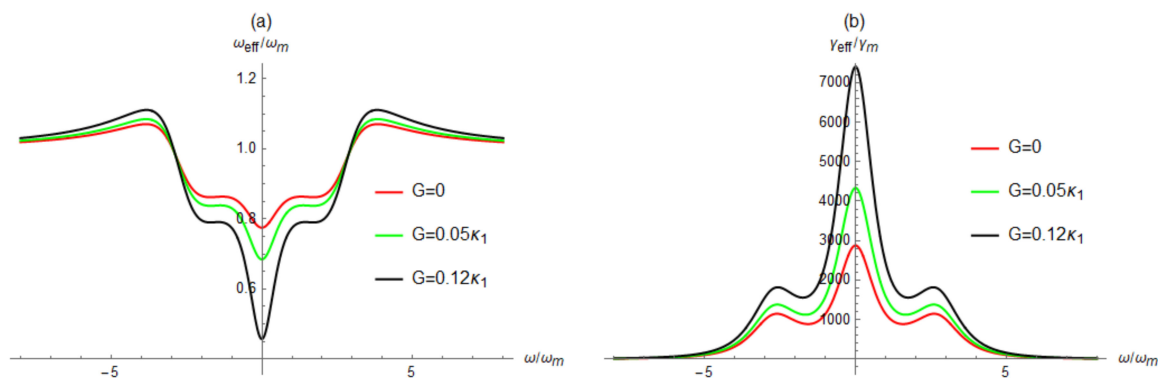


Figure 3. (a) The normalized effective resonance frequency $\omega_{eff}(\omega)/\omega_m$ of the mechanical oscillator as a function of the normalized frequency ω/ω_m for different parametric gains G ; (b) the normalized effective damping rate $\gamma_{eff}(\omega)/\gamma_m$ of the mechanical oscillator as a function of the normalized frequency ω/ω_m . The red curve, green curve, and black curve correspond to $G = 0$, $G = 0.05\kappa_1$, and $G = 0.12\kappa_1$, respectively. Where $\Delta = 0.9\omega_m$, $\Delta_2 = 2\omega_m$, $J = 1.25\kappa_1$, and $\theta = 0$.

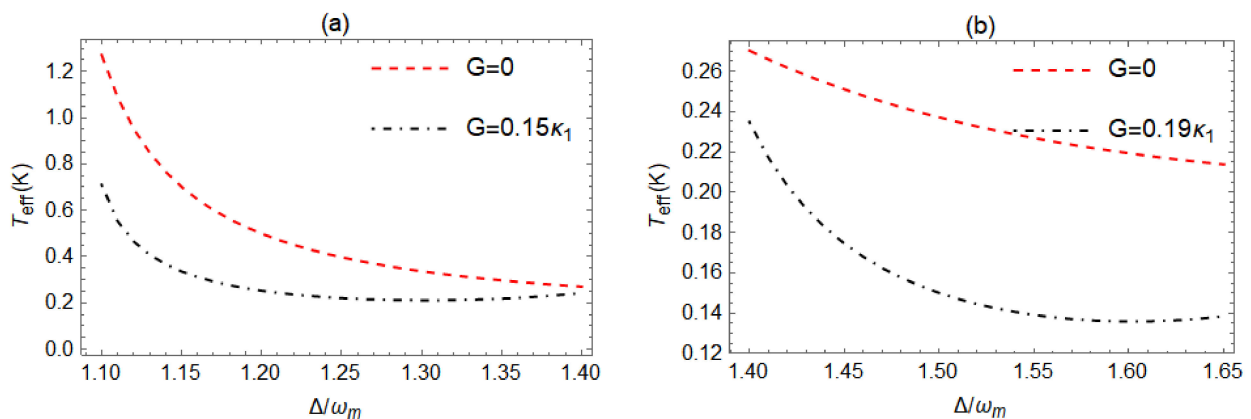


Figure 4. The effective temperature $T_{eff}(K)$ of the mechanical oscillator as a function of the normalized detuning Δ/ω_m of cavity a_1 for different parameter gains G : (a) $G = 0$ (red dashed curve), $0.15\kappa_1$ (black dot-dashed curve); (b) $G = 0$ (red dashed curve), $0.19\kappa_1$ (black dot-dashed curve). Where $J = 1.5\kappa_1$.

It can be seen that when the parameter gain G exists, the effective temperature of the mechanical oscillator is significantly improved. As the parameter gain increases, the cooling effect of the mechanical oscillator becomes more obvious, and the oscillator has a lower temperature. Furthermore, for the different parametric gain, the process of cooling corresponds to different ranges of the detuning of the effective cavity. For the parametric gain $G = 0.15\kappa_1$, the temperature can drop to $0.212K$, when $\Delta = 1.35\omega_m$. For the parametric gain $G = 0.19\kappa_1$, the effective temperature can arrive at $0.135K$, when $\Delta = 1.6\omega_m$. Similarly, we also plotted the effective temperature with or without the parametric gain G , when $J = 1.25\kappa_1$ and $J = \kappa_1$, as shown in Figure 5.

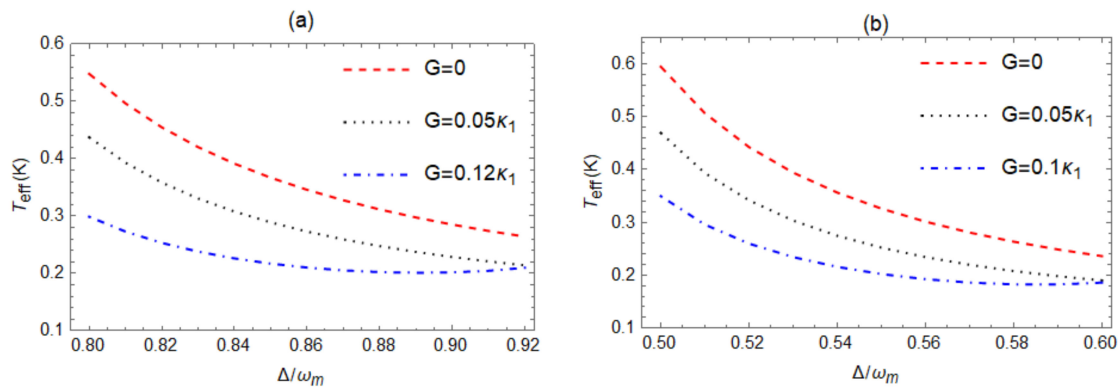


Figure 5. The effective temperature $T_{eff}(K)$ of the mechanical oscillator as a function of the normalized detuning Δ/ω_m of cavity a_1 for different parameter gain $G = 0$ (red dashed curve), $0.05\kappa_1$ (black dotted curve), $0.12\kappa_1$ (blue dot-dashed curve). Where $J = 1.25\kappa_1$ for (a) and $J = \kappa_1$ for (b).

According to the normalized effective mechanical damping $\gamma_{eff}(\omega)/\gamma_m$ in Figures 2 and 3, we can know that $\gamma_{eff}(\omega)/\gamma_m$ significantly increases when a parametric gain G is introduced, which means that the damping feedback force on the mechanical oscillator increases; thus, adding OPA can improve the cooling of the mechanical oscillator. In Figure 5a, when $J = 1.25\kappa_1$ and $\Delta = 0.8\omega_m$, then, $G = 0$, $G = 0.05\kappa_1$, and $G = 0.12\kappa_1$, the effective temperature of the mechanical oscillator is $0.548K$, $0.437K$, and $0.298K$, respectively. When $J = \kappa_1$ and $\Delta = 0.5\omega_m$, then, $G = 0$, $G = 0.05\kappa_1$ and $G = 0.1\kappa_1$, the effective temperature of the mechanical oscillator is $0.594K$, $0.469K$, and $0.349K$, respectively.

In addition, we also discussed the effect of the decay rate of the right cavity on the mechanical oscillator cooling. In the case of $J = 1.25\kappa_1$, $G = 0$, and $J = 1.25\kappa_1$, $G = 0.05\kappa_1$, we chose parameter κ_2 with different values κ_1 , $1.5\kappa_1$, $2\kappa_1$, and explored the relationship between the temperature of the mechanical oscillator and normalized detuning Δ/ω_m of the left cavity, as shown in Figure 6. With the increase in the decay rate of the right cavity, the cooling of the mechanical oscillator became more obvious. In addition, with or without the existence of the parameter gain, the appearance of the lowest temperature corresponds to different detuning.

We found that with the increase of κ_2 , the cooling effect of the mechanical oscillator was enhanced. In the same way, we also found a similar rule in the case of $J = 1.5\kappa_1$, $G = 0$, and $J = 1.5\kappa_1$, $G = 0.15\kappa_1$, as shown in Figure 7. Under appropriate parameter choices, a lower temperature cooling process can be achieved when the decay rate of the right cavity gradually increases. From Figure 7a,b, in this case we can find that the presence of parametric gain has little effect on the cooling of the mechanical oscillator, and the minimum temperature for both processes is around $0.2K$. Comparing Figure 7 with Figure 6, the cooling process has a strong dependence on the coupling between the two cavities. In Figure 7, we chose a larger coupling between the two cavities, and the cooling effect was reduced, as shown in Figure 6, where the coupling between the two cavities demonstrates smaller values. Thus, the parameter choices during the cooling process are very strict.

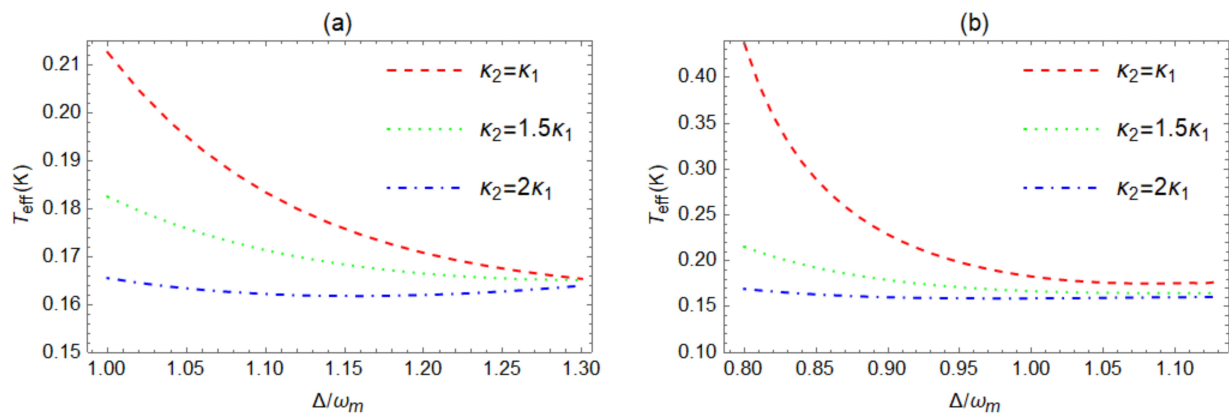


Figure 6. The effective temperature $T_{eff}(K)$ of the mechanical oscillator as a function of the normalized detuning Δ/ω_m of cavity a_1 for different decay rates of the right cavity $\kappa_2 = \kappa_1$ (red dashed curve), $1.5\kappa_1$ (green dotted curve), $2\kappa_1$ (blue dot-dashed curve). Where (a): $J = 1.25\kappa_1, G = 0$; (b): $J = 1.25\kappa_1, G = 0.05\kappa_1$.

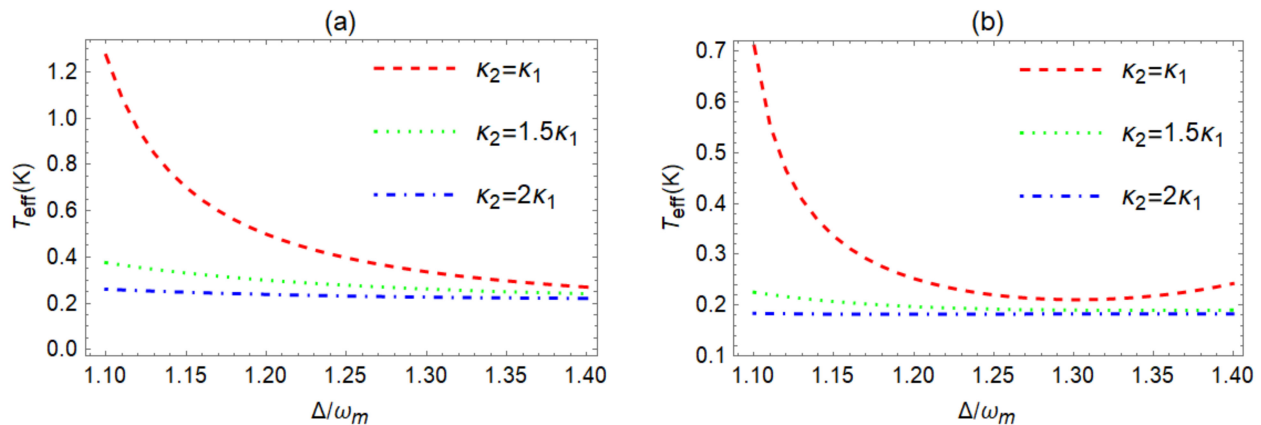


Figure 7. The effective temperature $T_{eff}(K)$ of the mechanical oscillator as a function of the normalized detuning Δ/ω_m of cavity a_1 for different decay rates of the right cavity $\kappa_2 = \kappa_1$ (red dashed curve), $1.5\kappa_1$ (green dotted curve), $2\kappa_1$ (blue dot-dashed curve). Where (a): $J = 1.5\kappa_1, G = 0$; (b): $J = 1.5\kappa_1, G = 0.15\kappa_1$.

5. Conclusions

In conclusion, we investigated mechanical oscillator cooling in two optical cavities, where one optical cavity is an optomechanical system and the other is a standard optical cavity. Photon exchange coupling existed between the two cavities. In addition, we placed an optical parametric amplifier in the left cavity. When the optomechanical system is driven by an input laser, we discussed the cooling of the mechanical oscillator under this condition using different parameters. Our study shows that we can improve the cooling effect of the mechanical oscillator under unresolved conditions. For appropriate physical parameters, we demonstrated that the cooling effect of the mechanical oscillator can also be improved with an increase in the gain factor of the optical parametric amplifier. In addition, we can also see that the mechanical oscillator can be cooled to a lower temperature by adjusting the decay rate of the right cavity. Our studies show that the photon exchange coupling between two cavities can also affect the cooling of the mechanical oscillator. Recently, with the development of micro/nano-processing technology, the experimental progress of cavity optomechanical systems has also developed rapidly [2–5], which provides an ideal platform for the study of quantum nonlinear phenomena in cavity optomechanical systems. A scheme for cooling the mechanical resonator close to its ground state, via an electromagnetically-induced-transparency-like mechanism in a double-cavity optome-

chanical system is proposed in ref. [31]. Our theoretical model is based on these research developments; therefore, our study has feasibility in these experiments.

Author Contributions: Conceptualization, software, formal analysis, writing—original draft preparation, P.P.; writing—review and editing, supervision, project administration, A.C. and L.D.; funding acquisition, A.C. All authors have read and agreed to the published version of the manuscript.

Funding: This research was supported by the National Natural Science Foundation of China through Grants No. 12175199, and No. 12174344, Zhejiang Provincial Natural Science Foundation of China through Grant No. LZ20A040002, and No. LY21A040007, and the Science Foundation of Zhejiang Sci-Tech University through Grants No. 19062408-Y and No. 17062071-Y.

Data Availability Statement: Not applicable.

Conflicts of Interest: The authors declare no conflict of interest.

References

1. Aspelmeyer, M.; Kippenberg, T.J.; Marquardt, F. Cavity optomechanics. *Rev. Mod. Phys.* **2014**, *86*, 1391–1452. [[CrossRef](#)]
2. Kippenberg, T.J.; Vahala, K.J. Cavity optomechanics: Back-action at the mesoscale. *Science* **2008**, *321*, 1172–1176. [[CrossRef](#)] [[PubMed](#)]
3. Sawadsky, A.; Kaufer, H.; Nia, R.M.; Tarabrin, S.P.; Khalili, F.Y.; Hammerer, K.; Schnabel, R. Observation of generalized optomechanical coupling and cooling on cavity resonance. *Phys. Rev. Lett.* **2015**, *114*, 043601. [[CrossRef](#)] [[PubMed](#)]
4. Cleland, A.N.; Geller, M.R. Superconducting qubit storage and entanglement with nanomechanical resonators. *Phys. Rev. Lett.* **2004**, *93*, 070501. [[CrossRef](#)] [[PubMed](#)]
5. Kotler, S.; Peterson, A.G.; Shojaee, E.; Lecocq, F.; Cicak, K.; Kwiatkowski, A.; Geller, S.; Glancy, S.; Knill, E.; Simmonds, W.R.; et al. Direct observation of deterministic macroscopic entanglement. *Science* **2021**, *372*, 622. [[CrossRef](#)]
6. Tetard, L.; Passian, A.; Venmar, K.T.; Lynch, R.M.; Voy, B.H.; Shekhawat, G.; Dravid, V.P.; Thundat, T. Imaging nanoparticles in cells by nanomechanical holography. *Nat. Nanotechnol.* **2008**, *3*, 501–505. [[CrossRef](#)]
7. Clerk, A.A.; Marquardt, F.; Jacobs, K. Back-action evasion and squeezing of a mechanical resonator using a cavity detector. *New J. Phys.* **2008**, *10*, 095010. [[CrossRef](#)]
8. Wollman, E.E.; Lei, C.U.; Weinstein, A.J.; Suh, J.; Kronwald, A.; Marquardt, F.; Clerk, A.A.; Schwab, K.C. Quantum squeezing of motion in a mechanical resonator. *Science* **2015**, *349*, 952–955. [[CrossRef](#)]
9. LaHaye, M.D.; Buu, O.; Camarota, B.; Schwab, K.C. Approaching the quantum limit of a nanomechanical resonator. *Science* **2004**, *304*, 74–77. [[CrossRef](#)]
10. Zheng, S.B.; Guo, G.C. Efficient scheme for two-atom entanglement and quantum information processing in cavity QED. *Phys. Rev. Lett.* **2000**, *85*, 2392–2395. [[CrossRef](#)]
11. Bassi, A.; Ippoliti, E.; Adler, S.L. Towards quantum superpositions of a mirror: An exact open systems analysis. *Phys. Rev. Lett.* **2005**, *94*, 030401. [[CrossRef](#)]
12. Zeng, W.; Nie, W.J.; Li, L.; Chen, A.X. Ground-state cooling of a mechanical oscillator in a hybrid optomechanical system including an atomic ensemble. *Sci. Rep.* **2017**, *7*, 17258. [[CrossRef](#)] [[PubMed](#)]
13. Chen, X.; Liu, Y.C.; Peng, P.; Zhi, Y.Y.; Xiao, Y.F. Cooling of macroscopic mechanical resonators in hybrid atom-optomechanical systems. *Phys. Rev. A* **2015**, *92*, 033841. [[CrossRef](#)]
14. Chan, J.; Alegre, T.; Safavi-Naeini, A.H.; Hill, J.T.; Krause, A.; Groblacher, S.; Aspelmeyer, M.; Painter, O. Laser cooling of a nanomechanical oscillator into its quantum ground state. *Nature* **2011**, *478*, 89. [[CrossRef](#)] [[PubMed](#)]
15. Liu, Y.C.; Hu, Y.W.; Wei, W.C.; Xiao, Y.F. Review of cavity optomechanical cooling. *Chin. Phys. B* **2014**, *22*, 114213. [[CrossRef](#)]
16. Gigan, S.; Böhm, H.R.; Paternostro, M.; Blaser, F.; Langer, G.; Hertzberg, J.B.; Schwab, K.C.; Bäuerle, D.; Aspelmeyer, M.; Zeilinger, A. Self-cooling of a micromirror by radiation pressure. *Nature* **2006**, *444*, 67–70. [[CrossRef](#)]
17. Dantan, A.; Genes, C.; Vitali, D.; Pinard, M. Self-cooling of a movable mirror to the ground state using radiation pressure. *Phys. Rev. A* **2008**, *77*, 011804. [[CrossRef](#)]
18. Groblacher, S.; Gigan, S.; Böhm, H.R.; Zeilinger, A.; Aspelmeyer, M. Radiation-pressure self-cooling of a micromirror in a cryogenic environment. *Europhys. Lett.* **2008**, *81*, 54003. [[CrossRef](#)]
19. Barzanjeh, S.; Naderi, M.H.; Soltanolkotabi, M. Back-action ground-state cooling of a micromechanical membrane via intensity-dependent interaction. *Phys. Rev. A* **2011**, *84*, 023803. [[CrossRef](#)]
20. Arcizet, O.; Cohadon, P.F.; Briant, T.; Pinard, M.; Heidmann, A. Radiation-pressure cooling and optomechanical instability of a micromirror. *Nature* **2006**, *444*, 71–74. [[CrossRef](#)] [[PubMed](#)]
21. Schliesser, A.; Del’Haye, P.; Nooshi, N.; Vahala, K.J.; Kippenberg, T.J. Radiation pressure cooling of a micromechanical oscillator using dynamical backaction. *Phys. Rev. Lett.* **2006**, *97*, 243905. [[CrossRef](#)]
22. Asjad, M.; Abari, N.E.; Zippilli, S.; Vitali, D. Optomechanical cooling with intracavity squeezed light. *Opt. Express* **2019**, *27*, 32427–32444. [[CrossRef](#)]

23. Mancini, S.; Vitali, D.; Tombesi, P. Optomechanical cooling of a macroscopic oscillator by homodyne feedback. *Phys. Rev. Lett.* **1998**, *80*, 688. [[CrossRef](#)]
24. Arcizet, O.; Cohadon, P.F.; Briant, T.; Pinard, M.; Heidmann, A.; Mackowski, J.-M.; Michel, C.; Pinard, L.; François, O.; Rousseau, L. High-sensitivity optical monitoring of a micromechanical resonator with a quantum-limited optomechanical sensor. *Phys. Rev. Lett.* **2006**, *97*, 133601. [[CrossRef](#)]
25. Poggio, M.; Degen, C.L.; Mamin, H.J.; Rugar, D. Feedback cooling of a cantilever's fundamental mode below 5 mK. *Phys. Rev. Lett.* **2007**, *99*, 017201. [[CrossRef](#)] [[PubMed](#)]
26. Rossi, M.; Mason, D.; Chen, J.; Tsaturyan, Y.; Schliesser, A. Measurement-based quantum control of mechanical motion. *Nature* **2018**, *563*, 53. [[CrossRef](#)] [[PubMed](#)]
27. Corbitt, T.; Wipf, C.; Bodiya, T.; Ottaway, D.; Sigg, D.; Smith, N.; Whitcomb, S.; Mavalvala, N. Optical dilution and feedback cooling of a gram-scale oscillator to 6.9 mK. *Phys. Rev. Lett.* **2007**, *99*, 160801. [[CrossRef](#)]
28. Genes, C.; Vitali, D.; Tombesi, P.; Gigan, S.; Aspelmeyer, M. Ground-state cooling of a micromechanical oscillator: Comparing cold damping and cavity-assisted cooling schemes. *Phys. Rev. A* **2008**, *79*, 039903. [[CrossRef](#)]
29. Wilson-Rae, I.; Nooshi, N.; Zwerger, W.; Kippenberg, T.J. Theory of ground state cooling of a mechanical oscillator using dynamical backaction. *Phys. Rev. Lett.* **2007**, *99*, 093901. [[CrossRef](#)] [[PubMed](#)]
30. Marquardt, F.; Chen, J.P.; Clerk, A.A.; Girvin, S.M. Quantum theory of cavity-assisted sideband cooling of mechanical motion. *Phys. Rev. Lett.* **2007**, *99*, 093902. [[CrossRef](#)] [[PubMed](#)]
31. Guo, Y.J.; Li, K.; Nie, W.J.; Li, Y. Electromagnetically-induced-transparency-like ground-state cooling in a double-cavity optomechanical system. *Phys. Rev. A* **2014**, *90*, 053841. [[CrossRef](#)]
32. Liu, Y.C.; Xiao, Y.F.; Luan, X.S.; Gong, Q.H.; Wong, C.W. Coupled cavities for motional ground-state cooling and strong optomechanical coupling. *Phys. Rev. A* **2015**, *91*, 033818. [[CrossRef](#)]
33. Ye, X.Q.; Huang, S.M.; Deng, L.; Chen, A.X. Improving the stochastic feedback cooling of a mechanical oscillator using a degenerate parametric amplifier. *Photonics* **2022**, *9*, 264. [[CrossRef](#)]
34. Huang, S.M.; Agarwal, G.S. Enhancement of cavity cooling of a micromechanical mirror using parametric interactions. *Phys. Rev. A* **2009**, *79*, 013821. [[CrossRef](#)]
35. Huang, S.M.; Chen, A.X. Improving the cooling of a mechanical oscillator in a dissipative optomechanical system with an optical parametric amplifier. *Phys. Rev. A* **2018**, *98*, 063818. [[CrossRef](#)]
36. Lau, H.K.; Clerk, A.A. Ground-state cooling and high-fidelity quantum transduction via parametric driven bad-cavity optomechanics. *Phys. Rev. Lett.* **2020**, *124*, 103602. [[CrossRef](#)] [[PubMed](#)]
37. Gardiner, C.W.; Zoller, P. *Quantum Noise*; Springer: Berlin/Heidelberg, Germany, 1991; Available online: <https://link.springer.com/book/9783540665717> (accessed on 1 December 2020).
38. Giovannetti, V.; Vitali, D. Phase-noise measurement in a cavity with a movable mirror undergoing quantum Brownian motion. *Phys. Rev. A* **2001**, *63*, 023812. [[CrossRef](#)]
39. Dejesus, E.X.; Kaufman, C. Routh-Hurwitz criterion in the examination of eigenvalues of a system of nonlinear ordinary differential equations. *Phys. Rev. A* **1987**, *35*, 5288. [[CrossRef](#)]
40. Cohadon, P.F.; Heidmann, A.; Pinard, M. Cooling of a mirror by radiation pressure. *Phys. Rev. Lett.* **1999**, *83*, 3174. [[CrossRef](#)]

Disclaimer/Publisher's Note: The statements, opinions and data contained in all publications are solely those of the individual author(s) and contributor(s) and not of MDPI and/or the editor(s). MDPI and/or the editor(s) disclaim responsibility for any injury to people or property resulting from any ideas, methods, instructions or products referred to in the content.